Electronic Supplementary Information

Rational design of Au-NiO hierarchical structures with enhanced rate performance for supercapacitors

Baihua Qu,[+a] Lingling Hu,[+a] Yuejiao Chen,[a] Chengchao Li,[a] Qiuhong Li,[a] Yanguo Wang[ab], Weifeng Wei[c], Libao Chen[*a] and Taihong Wang[*a]

a. Key Laboratory for Micro-Nano Optoelectronic Devices of Ministry of Education, and State Key Laboratory for Chemo/Biosensing and Chemometrics, Hunan University, Changsha 410082, P. R. China.

E-mail: thwang@hnu.edu.cn; and lbchen@hnu.edu.cn

b. Institute of Physics, Chinese Academy of Sciences, P.O. Box 603, Beijing 100190, P. R. China.

c. State Key Laboratory for Powder Metallurgy, Central South University, Changsha 410083, P. R. China

Experimental

All chemicals used in this study were of analytical grade and were used without further purification. Typically, 1.5 g nickel nitrate hexahydrate and 3 g urea was dissolved in a 200 mL beaker containing 80 mL deionized water and 10 mL ethanol. The mixture solution was stirred for 20 min at room temperature to mix homogeneously light green transparent solution, which was then transferred into a 100 mL Teflon-lined stainless steel autoclave. The autoclave was sealed and maintained at 90 °C for 12 h, then cooled to room temperature naturally. The resulting light green solid precipitates were collected by centrifugation, washed with deionized water and ethanol for several times to remove the possible absorbed ions, and then dried at 60 °C for 4 h. The NiO nanostructures were obtained after annealing at 400 °C for 4 h. The 0.2 g obtained NiO nanostructures were dissolved in 120 mL of deionized water by ultrasonication (30 min), and then $HAuCl_4$ solution (2 mM, 30 mL) was added dropwise into the solution under magnetic stirring. After stirring for 10 min 0.15 g of sodium citrate was added into the above solution, which was heating in a bath at 95 °C for 1h. After cooled to the room temperature, the precipitates were collected by centrifugation, washed with deionized water and ethanol, dried in a vacuum oven at 60 °C for 4 h.

The crystal structures of the precursor and the final products were examined by powder X-ray diffraction (XRD, SIEMENS D5000 diffractometer with Cu-Kα irradiation (λ= 1.5418 Å)). The morphologies and microstructures of the samples were characterized by a scanning electron microscopy (SEM, Hitachi S-4800), transmission electron microscope (TEM, JEOL-2010), energy dispersive X-ray spectroscopy (EDX) mapping and selected area electron diffraction (SAED) were carried out on JEM-2100F (JEOL) system operating at 200 kV. Thermogravimetric analysis and differential scanning calorimetry (TGA-DSC) was carried out under an air atmosphere on a NETZSCH STA-409 PC thermal analyzer with a heating rate of 10 °C min^{-1} ranging from room temperature to 800°C.

The electrochemical measurements were carried out in a three-electrode electrochemical cell containing 2 M KOH aqueous solution as the electrolyte. A standard calomel electrode (SCE) was used as the reference

electrode and a Pt foil as the counter electrode. The working electrode was prepared by mixing 80 wt% of Au-NiO (or pure NiO), 10 wt% of carbon black and 10 wt% of polyvinylidene difluoride (PVDF, Aldrich). This mixture was then pressed onto the Ni foam electrode and dried at 80 °C in a vacuum over for 12 h. The loading amount of the electrode is about 0.8-1 mg/cm^2. The Cyclic voltammetry (CV) measurements and galvanostatic discharge-charge test was conducted in 2M KOH aqueous electrolyte between 0 and 0.45 V vs. SCE on a CHI660c electrochemical workstation (Chenhua, Shanghai). The electrochemical impedance spectroscopy (EIS) tests were made with a superimposed 5 mV sinusoidal voltage in the frequency range of 100 kHz-0.01 Hz. The specific capacitance (C), energy density (*E*) and power density (*P*) were calculated according to the following equations:

$$C = \frac{i \times t}{\Delta u \times m} \tag{S1}$$

$$E = \frac{1}{2} \times C \times \Delta u^2 \tag{S2}$$

$$P = \frac{E}{t} \tag{S3}$$

Where Δu is the potential (V), v is the potential scan rate (mV s^{-1}), i is the discharging current (A), t is discharge time (s), and m is the mass (g) of the NiO or Au-NiO on the electrode. The current density of A g^{-1}, is this based on the mass of NiO or Au-NiO electrodes.

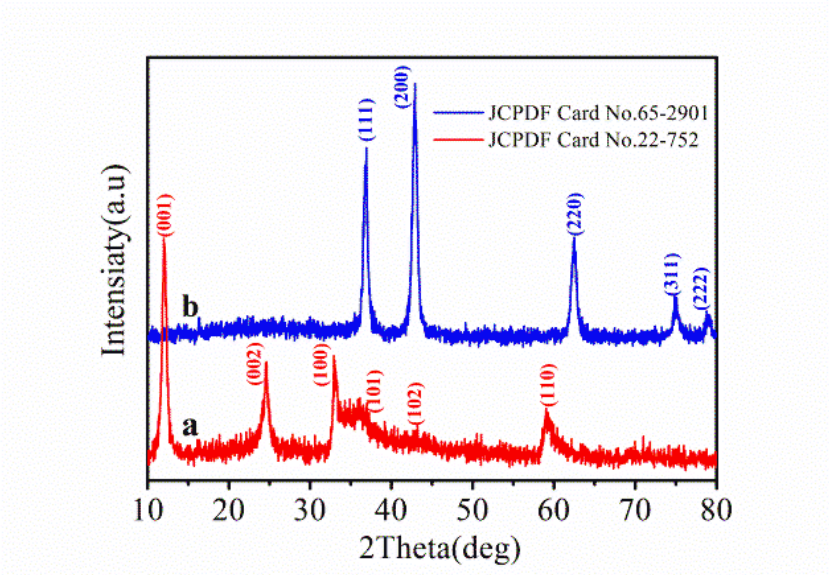

Fig. S1 XRD patterns of the precursor NiO nanoflakes material before (a) and after annealed in air at 400 °C for 4 h (b).

Fig.S1 showed the XRD patterns of the NiO precursor and the final product NiO. All the diffraction peaks of the precursor could be well indexed to $Ni_3(NO_3)_2(OH)_4$ of hexagonal structure (JCPDS No: 22-0752) (Fig. S1a). After heat treatment, strong and sharp diffraction peaks suggest the as-prepared products were well

crystallized. All the diffraction peaks were consistent with the face-centered cubic NiO phase (JCPDS Card no. 69-2901). TGA-DSC cure have further demonstrated $Ni_3(NO_3)_2(OH)_4$ precursor thermal decompose to porous NiO nanoflakes (Fig. S2). The total weight loss of $Ni_3(NO_3)_2(OH)_4$ was 33%, which was very close to the theoretical value (39.02%) calculated according to reaction: $2Ni_3(NO_3)_2(OH)_4 \rightarrow 6NiO + 4NO_2 + 4H_2O + O_2$. From SEM images (Fig. S3) shows many pores in the nanosheets, which could be attributed to the loss of volatile gas such as H_2O, O_2 and NO_2 during the heat treatment $Ni_3(NO_3)_2(OH)_4$ precursor.

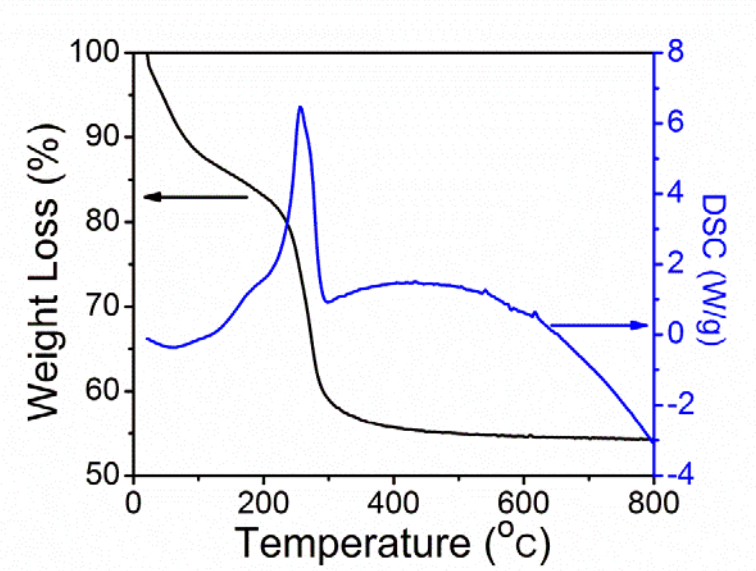

Fig. S2 TGA-DSC curves for the precursor NiO nanoflakes.

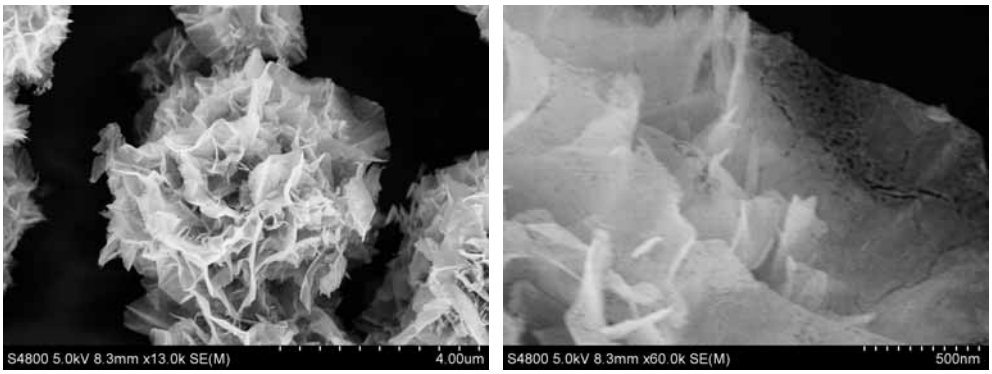

Fig. S3 SEM the NiO nanoflakes

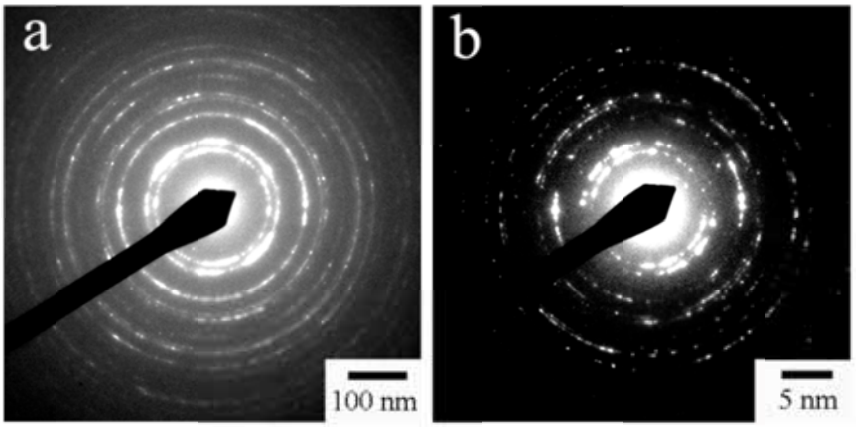

Fig. S4 SAED of (a) NiO nanoflakes and (b) Au-NiO hierarchical

The selective area electron diffraction (SAED) shown in Fig. S4 indicates a diffuse ring pattern, implying the existence of polycrystalline properties. In contrast, the Au-NiO in Fig. S2 (b) exhibited small and bright spot patterns on the diffuse ring. These results indicate that the Au nanoparticles in the Au-NiO might influence the growth orientation of NiO through interaction effects. A change of crystallinity in metal-incorporated NiO can affect the supercapacitor performance by changing the scattering path of the electrons. The excellent contact between the NiO and Au ligaments, as well as the detectable charge transfer, can significantly improve the electrical conductivity of the hybrid materials, as proved by the low internal resistance of the supercapacitor device.

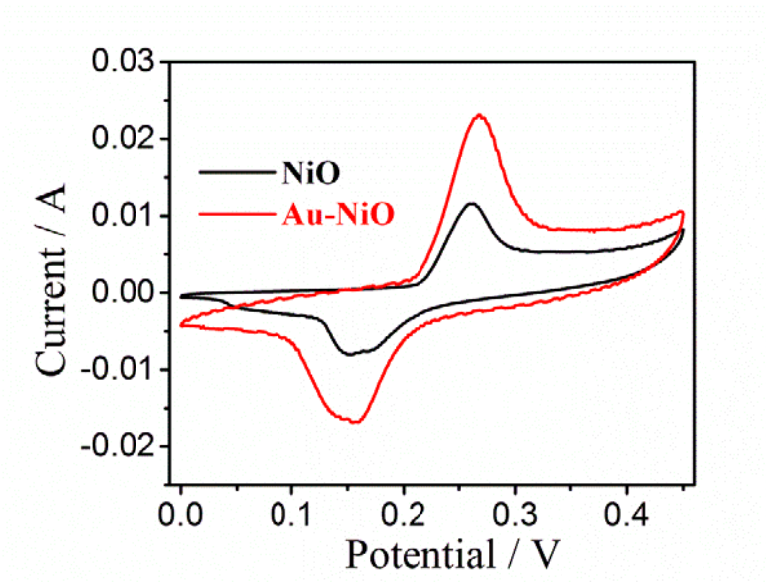

Fig. S5 Cyclic voltammetry (CV) curves of NiO and Au-NiO electrode at 10 mV s^{-1}

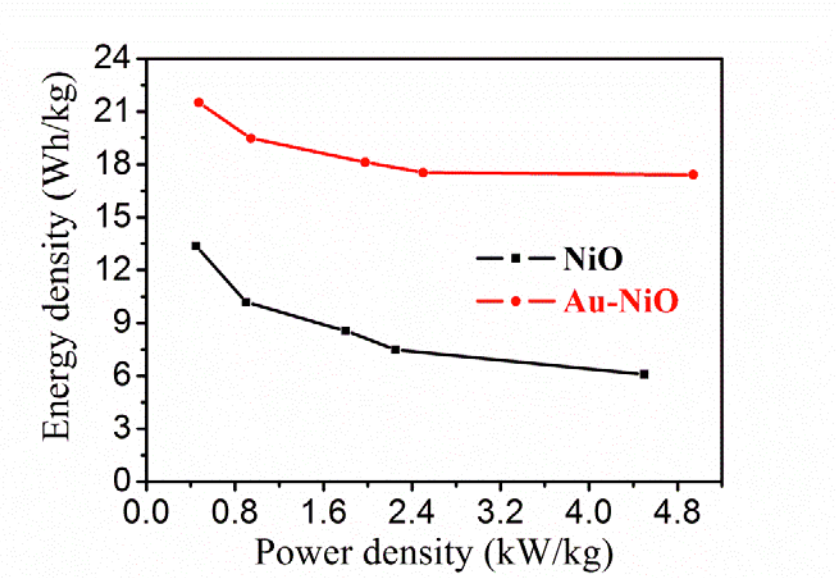

Fig. S6 Ragone plot of the estimated energy density and power density of NiO and Au-NiO electrode at various charge-discharge rates

The Ragone plot was estimated specific energy and specific power at the various current densities. As the galvanostatic charge-discharge current increased from 2 to 20 A g^{-1}. The energy densities of NiO electrode are 13.6, 10.2, 8.56, 7.48 and 6.08 Wh kg^{-1}, the specific powers of NiO electrode are 0.45, 0.9, 1.8, 2.25 and 4.5 kw kg^{-1} at current densities of 2, 4, 8, 10 and 20 A g^{-1}, respectively. While, the energy densities of Au-NiO electrode are 21.52, 19.48, 18.12, 17.53 and 17.41 Wh kg^{-1}, the specific powers of Au-NiO electrode are 0.47, 0.94, 1.98, 2.49 and 4.9 kw kg^{-1} at different current densities, respectively.

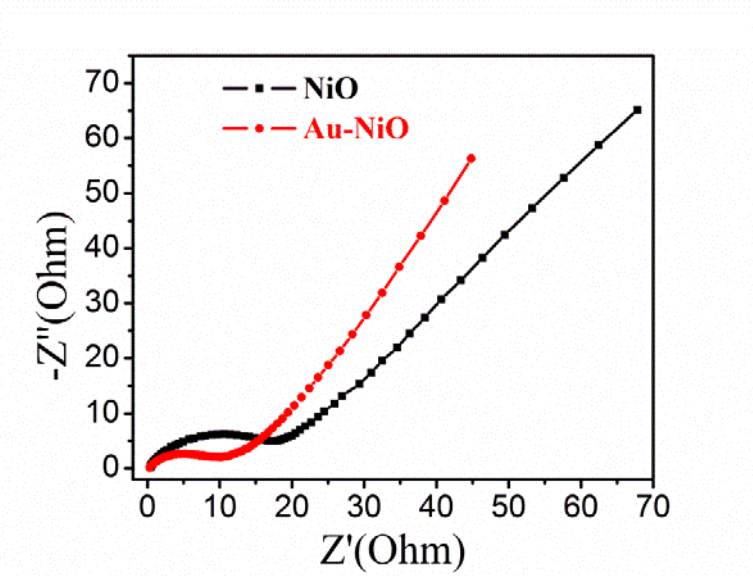

Fig. S7 EIS curves of NiO and Au-NiO electrode.